Zeitschrift für Physik A Manuscript-Nr.
(will be inserted by hand later)

Electromagnetic fission of ^{238}U at 600 and 1000 MeV per nucleon ⋆

Th. Rubehn[1], W. F. J. Müller[1], R. Bassini[2], M. Begemann-Blaich[1], Th. Blaich[3], A. Ferrero[2], C. Groß[1], G. Imme[4], I. Iori[2], G. J. Kunde[1] ⋆⋆, W. D. Kunze[1], V. Lindenstruth[1] ⋆⋆⋆, U. Lynen[1], T. Möhlenkamp[5], L. G. Moretto[6], B. Ocker[1], J. Pochodzalla[1], G. Raciti[4], S. Reito[4], H. Sann[1], A. Schüttauf[7], W. Seidel[5], V. Serfling[1], W. Trautmann[1], A. Trzcinski[8], G. Verde[4], A. Wörner[1], E. Zude[1], and B. Zwieglinski[8]

1 **Gesellschaft für Schwerionenforschung, D-64220 Darmstadt, Germany**
2 **Dipartimento di Fisica, Università di Milano and I.N.F.N., I-20133 Milano, Italy**
3 **Institut für Kernchemie, Universität Mainz, D-55099 Mainz, Germany**
4 **Dipartimento di Fisica dell' Università and I.N.F.N., I-95129 Catania, Italy**
5 **Forschungszentrum Rossendorf, D-01314 Dresden, Germany**
6 **Lawrence Berkeley Laboratory, Berkeley, CA 94720, USA**
7 **Institut für Kernphysik, Universität Frankfurt, D-60486 Frankfurt, Germany**
8 **Soltan Institute for Nuclear Studies, 00-681 Warsaw, Hoza 69, Poland**

Received: 8 May, 1995 / Accepted:

Abstract. Electromagnetic fission of ^{238}U projectiles at E/A = 600 and 1000 MeV was studied with the ALADIN spectrometer at the heavy-ion synchrotron SIS. Seven different targets (Be, C, Al, Cu, In, Au and U) were used. By considering only those fission events where the two charges added up to 92, most of the nuclear interactions were excluded. The nuclear contributions to the measured fission cross sections were determined by extrapolating from beryllium to the heavier targets with the concept of factorization. The obtained cross sections for electromagnetic fission are well reproduced by extended Weizsäcker-Williams calculations which include E1 and E2 excitations. The asymmetry of the fission fragments' charge distribution gives evidence for the excitation of the double giant-dipole resonance in uranium.

PACS: 25.75.+r, 25.85.–w, 27.90.+b

1 Introduction

In relativistic heavy-ion collisions, electromagnetic processes are expected to have large cross sections due to the fast time variation of the electromagnetic field. The process of electromagnetic dissociation can occur if one of the nuclei is excited above its particle emission threshold. It may then deexcite by particle emission or, if the excitation energy is above the fission threshold, by fission. The latter process is called electromagnetic fission. A framework for the calculation of electromagnetic dissociation cross sections is given by the Weizsäcker-Williams (WW) approximation folded with experimental photoabsorption cross sections [1].

Electromagnetic dissociation was first observed in cosmic ray experiments [2] and in projectile fragmentation of ^{12}C and ^{16}O by Heckman and Lindstrom [3]. Further experiments gave evidence for electromagnetic dissociation in the fragmentation of ^{18}O projectiles at E/A = 1.7 GeV [4] and of ^{197}Au targets excited by various projectiles [5, 6]. Electromagnetic multiphonon excitations of the same targets were studied measuring the 1n, 2n and 3n removal cross sections [7, 8]. In other experimtents the γ-ray and neutron decay of the electromagnetically excited double giant-dipole resonance (GDR) in ^{208}Pb and ^{136}Xe was observed [9, 10, 11]. While the 1-phonon excitations were well reproduced by the calculations, the cross sections of the 2-phonon excitations were underpredicted [12, 13]. In a recent experiment 1n to 4n removal cross sections of ^{238}U-projectiles impinging on Al, Cu and Pb targets were measured [14]. The results were well reproduced by WW-calculations including the excitation of the double GDR.

Experimental studies have, in particular, shown that fission of ^{238}U at relativistic energies can be a result of electromagnetic interactions, presumably via the excitation of the giant-dipole resonance. Jain et al. investigated the fission of uranium projectiles at E/A = 960 MeV in nuclear emulsions [15]. "Clean" fission events consisting of only two fission fragments with no other charged particle or target fragmentation tracks were observed. Fission cross sections of ^{238}U-projectiles at E/A = 900 MeV after collisions with H to Pb targets were reported by Greiner et al. [16]. Since the target dependence could not be explained by an increase of the geometrical cross section only, a contribution from electromagnetic fission was assumed. Schmidt et al. [17] and Bernas et al. [18] measured charge spectra of fission fragments from ^{238}U-projectiles hitting a lead target. In addition to the symmetric component of the spectra an asymmetric contribution was found which was assumed to be due to electromagnetic excitations. In an experiment performed at the BEVALAC, electromagnetic fission of ^{238}U at E/A = 120 MeV was studied using various targets [19]. The nuclear contributions were determined by scaling the data for a Be target according to a geometrical model. A qualitative agreement between the experimental cross sections and the results of Weizsäcker-Williams calculations was found. Recently, electromagnetic fission of uranium was reported for Pb-projectiles at E/A = 100, 500, 1000 MeV [20]. The authors disentangled the nuclear and the electromagnetic contribution on the basis of their different angular distributions. Within the uncertainties of the method the cross sections for electromagnetic fission are in good agreement with WW calculations including E1, E2 and the possibility of 2-phonon excitations. In the literature, how-

⋆ This work forms part of the Ph.D. thesis of Th. Rubehn.
⋆⋆ *Present address:* NSCL, MSU, East Lansing, MI 48824, USA
⋆⋆⋆ *Present address:* LBL, Berkeley, CA 94720, USA

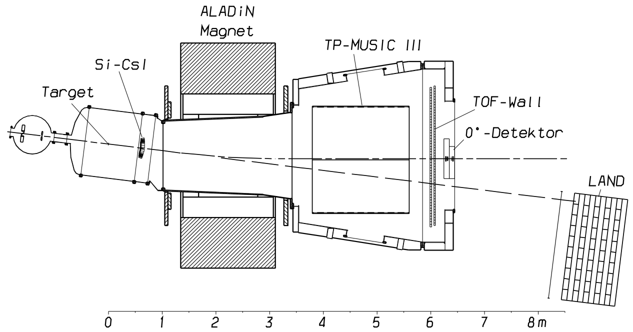

Fig. 1. Schematic view of the ALADIN facility. The beam entered from the left, projectile fragments were tracked and identified in the MUSIC detector and in the time-of-flight (TOF) wall. Coincident neutrons emitted approximately in the direction of the incident beam were detected by the LAND detector. The multiplicity of light particles emitted from the interaction zone was measured using the Si-CsI hodoscope.

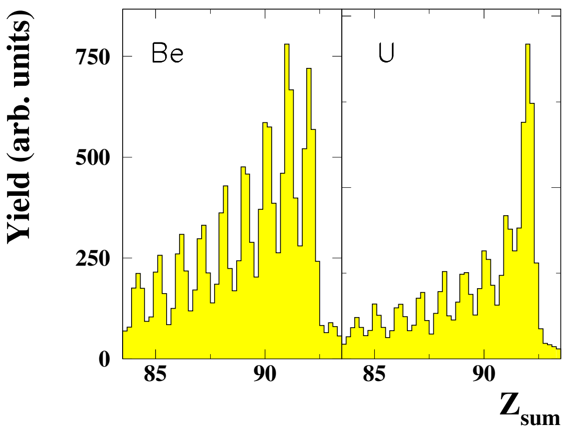

Fig. 2. Spectrum of the charge sum Z_{sum} of the fission fragments for the reactions ^{238}U on Be and U at E/A = 1000 MeV.

ever, only little information can be found which shows more than a qualitative agreement between the experimental results and the WW calculations.

In order to test the validity of the theoretical description more precisely, it is necessary to determine the target and energy dependence of the cross sections with a better accuracy than hitherto reported. In this paper we present cross sections for electromagnetic fission of uranium at E/A = 600 and 1000 MeV for several targets. Individual charge resolution was achieved for both fission fragments. Therefore, an efficient selection of electromagnetic fission events was made possible by requiring that the sum of the fission fragments' charges equaled 92. Conversely, a major part of the nuclear interactions were identified by the detection of charged particles emitted from the interaction zone.

2 Experiment

Fission of ^{238}U-projectiles at incident energies of E/A = 600 and 1000 MeV after bombardment of seven different targets (Be, C, Al, Cu, In, Au, U) with a thickness between 185 and 800 mg/cm^2 was investigated using the ALADIN forward spectrometer [21] at the heavy-ion synchrotron SIS of GSI. Due to the high kinetic energy of the uranium beam the fragments of the projectile fission were emitted in a narrow cone close to the beam direction.

In Fig. 1, we show the experimental setup in a schematic view. For each projectile nucleus its position and arrival time were measured upstream of the target with two thin plastic scintillators. The projectile fragments were detected by the Time Projection Multiple Sampling Ionization Chamber (MUSIC) and by the time-of-flight wall (TOF) positioned behind the dipole magnet. A set of 18 multiwire proportional counters and 48 anode strips allowed the measurement of the atomic numbers for fragments from He to U together with their positions and angles. A resolution of 0.5 (FWHM) was achieved for the charge sum of the fission fragments (see Fig. 2). The TOF wall consisted of 192 scintillator strips arranged in two layers. Light particles and fragments emitted at Θ_{Lab} between 5 and 17 degrees were detected in a hodoscope of 84 Si-CsI telescopes. Coincident neutrons were measured with the LAND detector [22] positioned behind the ALADIN spectrometer. In this paper we will not make use of the neutron data, however.

At beam energies of E/A = 600 and 1000 MeV, fission fragments are, with respect to the beam axis, emitted into a cone of polar angles of 2.1 and 2.9 degree, respectively. This is well within the acceptance of the ALADIN spectrometer of $\pm 9.2^0$ in horizontal and $\pm 4.3^0$ in vertical direction. Due to the finite double-hit resolution in the MUSIC the detection efficiency was limited to 87% at E/A = 600 MeV and 81% at 1000 MeV. The cross sections were corrected for this effect. For this correction the angular distribution of the fission fragments was assumed to be isotropic in the CM-system. This assumption is, however, not crucial since anisotropy coefficients of $a = 0.4 - 0.5$ in the distribution $W(\theta) = 1 \pm a \cos^2\theta$, as reported for a narrow energy window in photofission experiments with monochromatic gamma rays [23], would change the efficiency only by 1%.

3 Calculations

Electromagnetic dissociation processes are usually described by replacing the electromagnetic field by an equivalent photon flux. The absorption of a virtual photon will excite the nucleus which can then dissociate according to the branching ratios of the particular channel. The Weizsäcker-Williams description [24, 25, 26] of the photon spectrum was extended by including higher multipolarities $\pi\, l$ [27]. The cross section of electromagnetic dissociation into a specific channel Ψ can be expressed by:

$$\sigma_{emd}^{\Psi} = \sum_{\pi\, l} \int \sigma_{\gamma,\Psi}^{\pi\, l}(\omega)\; N^{\pi\, l}(\omega)\; d\omega, \qquad (1)$$

where ω is the energy of the photon, σ_γ is the photodissociation cross section and $N(\omega)$ is the photon spectrum generated by the collision partner.

The E1 and E2 spectra integrated over the impact parameter are given by

$$N^{E1}(\omega) = \frac{2Z^2\alpha}{\pi\omega\beta^2}\left(\xi K_0(\xi)K_1(\xi) - \frac{\beta^2\xi^2}{2}\left(K_1^2(\xi) - K_0^2(\xi)\right)\right) \qquad (2)$$

and

$$N^{E2}(\omega) = \frac{2Z^2\alpha}{\pi\omega\beta^4}\left(2\left(1-\beta^2\right)K_1^2(\xi) + \left(2-\beta^2\right)^2 \times \xi K_0(\xi)K_1(\xi) - \frac{\xi^2\beta^4}{2}\left(K_1^2(\xi) - K_0^2(\xi)\right)\right), \quad (3)$$

where Z is the charge and β the velocity of the particle, α the fine structure constant, K_0 and K_1 are modified Bessel functions and $\xi = \omega b_{min}/(\beta\gamma)$. b_{min} is the cutoff impact parameter below which nuclear processes take over and become dominant. Higher multipolarities turn out to be less important in our case since their effect is much smaller than the error bars of the experiment [28]. $N^{E1}(\omega)$ is identical with the photon spectrum of the simple Weizsäcker-Williams theory [27]. The photofission cross section can then be expressed as

$$\sigma_{\gamma,f}(\omega) = \sigma_{\gamma,tot}(\omega)P_f(\omega), \quad (4)$$

where P_f is the fission probability. In our calculations Lorentz parametrizations of the total photo cross section for the GDR were taken from Ref. [29] which are in good agreement with other measurements [23, 30, 31, 32]. Furthermore, we used the parametrizations for the isoscalar component of the GQR from Ref. [31] and for the isovector component from Ref. [33]. The fission probability P_f is known up to $\approx$ 20 MeV [29, 34]. For higher excitation energies the Γ_n/Γ_f ratios were determined using the results of an evaporation calculation [35].

Llope and Braun-Munzinger developed a framework for a quantitative analysis including the multiple excitation of the giant resonances [36] describing the excitation process as a single or multiple excitation of a classical harmonic oscillator [37, 27]. The probability density for multiple excitations can be achieved by a repeated folding of the probability for the absorption of single photons at a fixed impact parameter. After the integration over all impact parameters, the cross section can be expressed as:

$$\sigma_{n-phonon} = \int dE^*\left(\frac{d\sigma^{(1)}}{dE^*} + \frac{d\sigma^{(2)}}{dE^*} + \ldots\right), \quad (5)$$

where $d\sigma^{(1)}/dE^*$ and $d\sigma^{(2)}/dE^*$ are the contributions from single and double phonon excitations, respectively. Comparisons between calculations which allow 1-phonon excitations only and those including the excitation of the double GDR show insignificantly small differences of the cross sections for electromagnetic fission. This is due to the fact that the higher fission probability in the energy regime of the double GDR is to a large extent compensated by the redistribution of cross section from one phonon to that of two phonon excitation. Therefore, the results of the calculations are independent of the strength of the double GDR as long as electromagnetic fission cross sections are discussed. This, however, is not true for quantities which are sensitive to the excitation energy distribution, i.e. the proton odd-even-effect and the asymmetry of the fission fragments' charge distribution.

In the extended WW calculations we used different parametrizations for the cutoff parameter b_{min}. Benesh, Cook and Vary (BCV) proposed the dependence [38]

$$b_{min}^{BCV} = r_0\left(A_p^{1/3} + A_t^{1/3} - x\left(A_p^{-1/3} + A_t^{-1/3}\right)\right), \quad (6)$$

where A_p and A_t are the masses of the target and projectile nuclei, r_0 = 1.34 fm and x = 0.75. This parametrization was obtained from a fit of the results of a Glauber calculation. Another parametrization which gives a very good overall description of experimental reaction cross sections for medium-heavy nuclei at medium and high energies has been developed by Kox et al. [39]

$$b_{min}^{Kox} = r_0\left(A_p^{1/3} + A_t^{1/3} + a_0\frac{A_p^{1/3}A_t^{1/3}}{A_p^{1/3} + A_t^{1/3}} - c\right), \quad (7)$$

where r_0=1.1 fm, a_0=1.85 and c is an energy dependent correction term. The existing measurements of the total reaction cross sections for heavy systems are, however, not sufficiently precise to allow a final decision in favour of one of the parametrizations.

In a recent work Aumann, Bertulani and Sümmerer developed a microscopic approach to resolve the ambiguity connected with the choice of the cutoff parameter [12]. They compared the results obtained from a soft-spheres model with the sharp-cutoff results. The differences in the cross sections using the BCV parametrization and the soft-spheres model turned out to be insignificant.

In the WW calculation the assumption is made that all nuclei have a spherical shape. Bertulani showed that the averaging over the projectile orientation leads to a slight increase of the cross section. For the moderate deformation of uranium (β_{def}=0.3) the effect is, however, negligible [40].

4 Results and discussion

The total fission cross section contains both electromagnetic fission and nuclear interaction processes with possibly larger energy and/or charge transfer. Photofission experiments with uranium show that, averaged over the relevant range of excitation energies, the probability for the emission of light charged

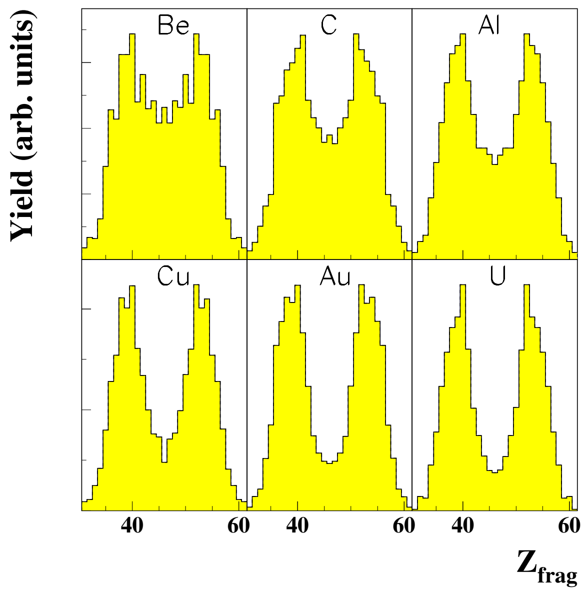

Fig. 3. Charge distributions of the fission fragments for several targets at E/A = 1000 MeV under the condition that the sum of the charges of the fission fragments equals 92 and that the multiplicity in the hodoscope is zero.

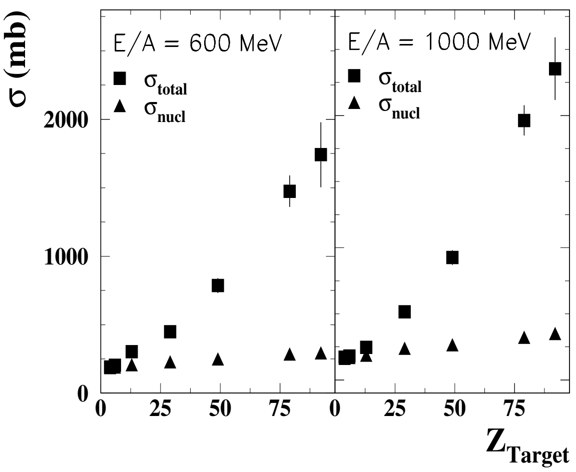

Fig. 4. Measured fission cross sections (squares) at E/A = 600 (left) and 1000 (right) MeV for the different targets under the conditions Z_{sum} = 92 and M_{hodo} = 0. The magnitude of the nuclear cross sections (triangles) was determined using the concept of factorization described in the text.

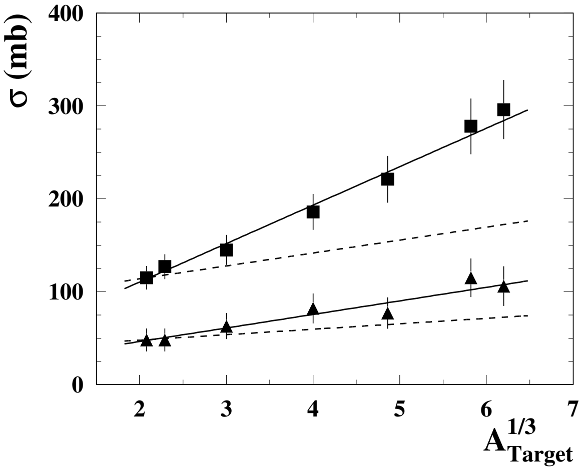

Fig. 5. Cross sections for those events where the sum of the charges of the fragments equals 90 (squares) and for those events where Z_{sum} = 92 but light particles were detected in the hodoscope (triangles). The dashed line shows the results of the geometrical model, fitted to beryllium, while the solid lines represent straight line fits to the data.

particles is in the order of 10^{-3} [41]. Therefore, electromagnetic fission events could be enriched by the condition that the sum of the charges of the fission fragments equaled 92. To further reduce the nuclear contribution we required that the multiplicity M_{hodo} observed in the Si-CsI hodoscope was zero. With the beryllium target, these two conditions allow to reject 80% of the observed fission events.

The cross sections had to be corrected for nuclear interactions of the fragments in the target and in the material of the detectors. To determine this effect experimental total charge changing cross sections for various systems were used [43, 44, 45] and interpolations for typical fission fragments were made. The difference to calculated total reaction cross sections was used as an estimate of the associated uncertainty.

In Fig. 3, we show inclusive charge spectra of the fission fragments for different targets under the previously described conditions. A transition to more asymmetric fission can be observed as the atomic number of the target increases. Since for pure electromagnetic fission no target dependence of the asymmetry would be expected, the observed increase indicates an additional contribution with a different dependence on the atomic number of the target; this component is due to nuclear collisions. From light particle induced fission of ^{238}U it is well known that the asymmetry in the charge spectrum of the fission fragments is a sensitive measure of the excitation energy imparted to the system [42], higher excitation energies lead to more symmetric fission. The excitation energies of electromagnetic fission are dominated by the GDR located at ~12 MeV and should, therefore, lead to asymmetric fission. Since the ratio between electromagnetic and nuclear fragmentation is expected to increase with the charge of the target ($\sigma_{emd} \propto Z^{1.8}_{Target}$) the experimentally oberserved decrease of the mean excitation energy can be understood.

The efficiency corrected experimental fission cross sections for those events where Z_{sum} = 92 and M_{hodo} = 0 are plotted in Fig. 4. A much stronger increase with the atomic number of the target can be seen than it would be expected for nuclear processes. The observed transition to more asymmetric fission and the dependence of the measured total cross section on the charge of the target indicates a dominant contribution of the electromagnetic excitation for the heavy targets.

The total cross section can be expressed as the sum of the cross sections for electromagnetic and peripheral nuclear processes:

$$\sigma_{total} = \sigma_{EMF} + \sigma_{nuclear}. \tag{8}$$

The determination of the nuclear contributions starts from the assumption that the total cross section measured for the Be target is almost entirely due to nuclear processes. Two different methods, a geometrical model [19, 38] and the concept of factorization [3, 46], were investigated to extrapolate the nuclear contributions for the heavier targets.

The picture of the geometrical model assumes that only the most peripheral collisions contribute to the nuclear fission cross section and therefore only reactions with impact parameters from b_{min} to a slightly smaller impact parameter $b_{min} - \Delta b$ are taken into account. Here, b_{min} is the impact parameter where the surfaces of the colliding nuclei begin to touch. In this model Δb is assumed to be independent of the target. The nuclear cross section can then be written as

$$\sigma^{geom}_{nuclear} = 2\pi \left(b_{min} - a - \frac{\Delta\, b}{2} \right) \Delta\, b \tag{9}$$

where $a = \frac{Z_p Z_t e^2}{\mu \beta^2 \gamma}$ corrects for the Rutherford bending of the trajectory [19].

In Fig. 5, the predictions of the geometrical model are compared to the cross sections for those events where the sum of the fragment charges equals 90 and those events where Z_{sum} = 92 but at least one light charged particle was detected in the hodoscope; these events are due to strong interactions. Eq. (9) was adjusted to reproduce the cross sections for the Be target. The observed target dependence is stronger than predicted by geometrical model calculations. Therefore, the following alternative method was applied.

On the assumption that projectile fragmentation in peripheral nuclear collisions can be considered as a two-step process,

Table 1. Experimental cross sections σ_{EMF} in mb for electromagnetic fission of ^{238}U at 600 and 1000 MeV per nucleon. For the results of the WW calculations using the BCV parametrization for the cutoff parameter σ_{WW}^{BCV} the contribution from the E1 and E2 excitations are shown. For comparison we give the calculated cross sections using the Kox parametrization for b_{min}. Both the statistical and the systematical errors are given.

Target	E/A = 1000 MeV σ_{EMF}	σ_{WW}^{BCV}	σ_{WW}^{E1}	σ_{WW}^{E2}	σ_{WW}^{Kox}	E/A = 600 MeV σ_{EMF}	σ_{WW}^{BCV}	σ_{WW}^{E1}	σ_{WW}^{E2}	σ_{WW}^{Kox}
Be	7^a	7	6	1	7	6^a	6	5	1	7
C	$11 \pm 6 \pm 13$	15	13	2	15	$12 \pm 8 \pm 16$	14	11	3	14
Al	$61 \pm 7 \pm 15$	64	54	9	62	$97 \pm 13 \pm 18$	55	45	10	54
Cu	$277 \pm 14 \pm 28$	273	236	37	251	$218 \pm 16 \pm 27$	228	191	38	208
In	$666 \pm 20 \pm 56$	690	602	88	616	$541 \pm 26 \pm 57$	560	473	87	492
Au	$1644 \pm 25 \pm 118$	1577	1389	188	1376	$1192 \pm 40 \pm 94$	1240	1059	182	1056
U	$2007 \pm 52 \pm 234$	2036	1799	237	1764	$1449 \pm 27 \pm 112$	1581	1355	227	1333

^{a} The cross sections for beryllium are taken from WW-calculations as described in the text.

the production cross section σ_{PT}^F of a specific fragmentation channel can be described as a product of a formation cross section γ_T^P, depending on the target (T) and the projectile (P), and a branching ratio γ_P^F which depends on the projectile and the fragmentation channel. This leads to the widely used factorization ansatz $\sigma_{PT}^F = \gamma_P^F \gamma_T^P$ [3, 5, 6, 7, 46]. The cross section ratios for a given Target T, with respect to the Be target,

$$R_F(T) = \frac{\sigma_{U,T}^F}{\sigma_{U,Be}^F} = \frac{\gamma_T^U}{\gamma_{Be}^U} \tag{10}$$

should be independent of the fragmentation channel.

Other measurements with comparable systems show that peripheral nuclear fragmentation can be described by factorization [5, 6]. In order to verify the assumption, in particular, for fission resulting from nuclear collisions, we compare in Fig. 6 ratios of the cross sections for different targets obtained for several channels with $Z_{sum} < 92$. For a given target, the variances are small and the assumption of factorization for nuclear fission is therefore justified. The obtained ratios $R_F(T)$ were then used to determine the cross sections of nuclear fission for the various targets:

$$\sigma_{nucl}(T) = \left(\sigma_{total}(Be) - \sigma_{EMF}^{WW}(Be)\right) < R_F(T) > . \tag{11}$$

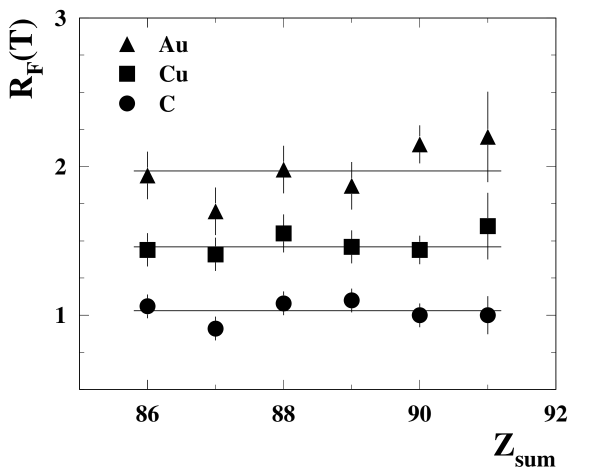

Fig. 6. Cross section ratios $R_F(T)$ for different targets as a function of the fission fragments' charge sum Z_{sum}.

The nuclear cross section for the beryllium target was determined by subtracting the cross section for electromagnetic fission of 6 and 7 mb, respectively, obtained from WW calculations, from the measured total cross sections of 167 and 190 mb. The results are shown in Fig. 4. The cross sections for electromagnetic fission determined by this method are listed in Tab. 1 and plotted in Fig. 7. Weizsäcker-Williams calculations using the BCV parametrization are in good agreement with the data while the results using the Kox parametrization give too low cross sections. We should note that the widely used parametrizations [1, 19, 20] of the experimental total photoabsorption cross section for the GDR from Livermore [34] are systematically higher than those of [29, 30, 31, 32] and lead to about 16% higher cross sections in the WW calculations [1, 19].

In Fig. 8 we combine the energy dependence of electromagnetic fission of ^{238}U after collisions with ^{208}Pb with cross sections obtained in other experiments at various energies between E/A = 100 and 1000 MeV. Since the results of [19] and our data were not achieved with a lead target a scaling from the uranium and the gold target, respectively, was made. The experimental data, except for the cross section of Polikanov

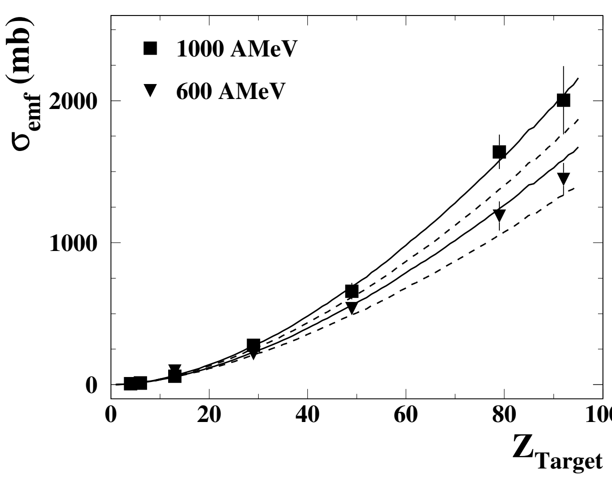

Fig. 7. Cross sections for electromagnetic fission of ^{238}U projectiles at E/A = 600 and 1000 MeV beam energy as a function of the atomic number Z of the target. The lines show the predictions of calculations based on the extended Weizsäcker-Williams theory using the BCV (full lines) and the Kox (dashed lines) parametrizations for the cutoff parameter.

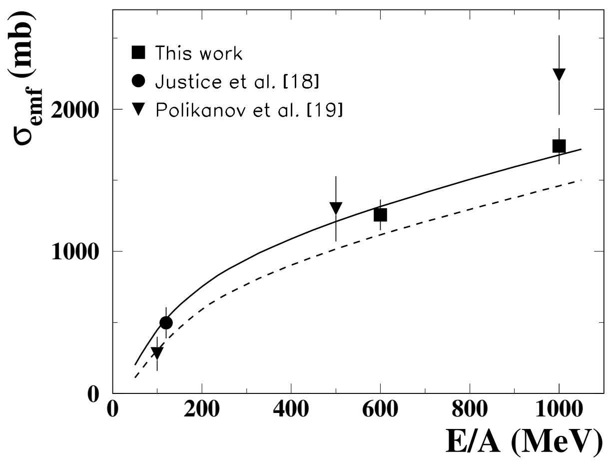

Fig. 8. The electromagnetic fission cross section as a function of the beam energy for the system ^{238}U + ^{208}Pb in comparison to the prediction of WW calculations using the BCV (solid line) and the Kox (dashed line) parametrizations.

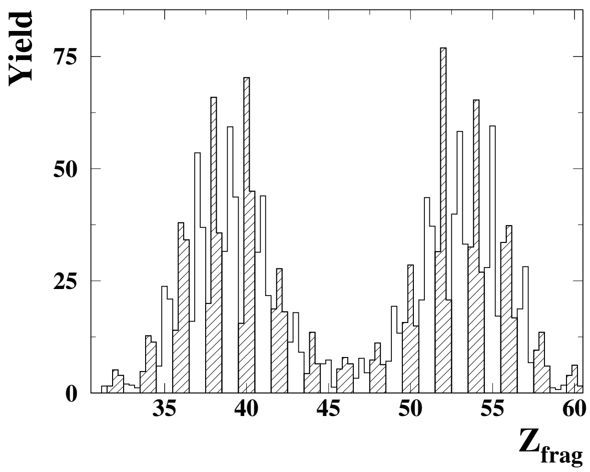

Fig. 10. Electromagnetic fission charge spectrum of the uranium target at E/A = 1000 MeV. The proton odd-even-effect is visible in the two peak regions.

et al. [20] at E/A = 1000 MeV, are well reproduced by the results of WW calculations using the BCV parametrization.

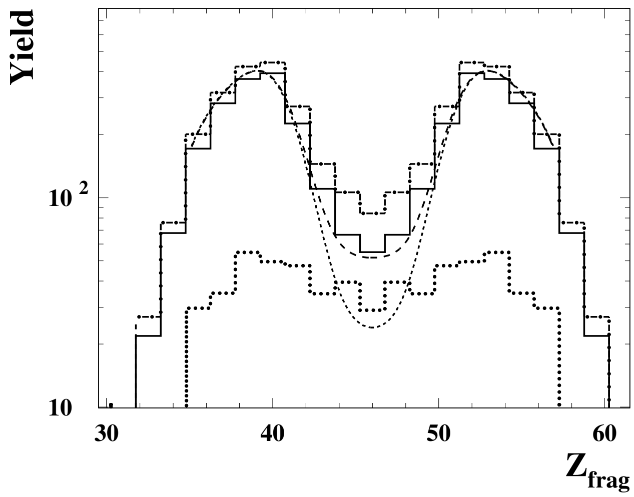

Fig. 9. Charge distributions of the fission fragments for the uranium target at E/A = 1000 MeV. The different histograms show the total measured spectrum (dashed-dotted line, same as in Fig. 3), the nuclear background (dotted line) and the resulting distribution for electromagnetic fission (full line). The smooth curves show the results of folding calculations excluding (short dashed line) and including the excitation of the double GDR (long dashed line).

Furthermore, we investigated the asymmetry of the fission fragments' charge spectrum and the proton odd-even-effect. The two observables are sensitive to the excitation energy of the fissioning nucleus. While the proton odd-even-effect represents a measure of low energy contributions, the peak-to-valley ratio predominantly reflects contributions from higher excitation energies.

The charge spectrum for electromagnetic fission was separated using exactly the same procedure as for the cross sections, i.e. the scaled beryllium spectrum was subtracted from the measured distribution. In Fig. 9, we show the experimental charge spectrum, the nuclear background and the resulting distribution due to electromagnetic fission. An experimental peak-to-valley ratio p of 7.2 ± 1.0 was observed for the uranium target at E/A = 1000 MeV.

An experimental proton odd-even-effect δ = $(7 \pm 1.5)\%$ was determined from integrating the cross sections of fragments with odd and even charge numbers. As shown in Fig. 10, the enhancement of the production of fragments with even nuclear charge numbers is barely visible in the peak region.

In order to understand the experimental results we investigated folding calculations including the excitation energy distribution of the WW-theory and the fission probability, parametrizations of experimental peak-to-valley ratios [47, 48, 49] and the proton odd-even-effect [50] as a function of the excitation energy. For energies below ∼15 MeV experimental fission probabilities were used [34], for higher excitation energies the results of a calculation [14]. The WW calculations were performed using the harmonic oscillator ansatz with ordinary strength for the excitation of the double GDR as described before.

On the assumption that the parametrization of the peak-to-valley ratio is also valid for neighbouring isotopes, experimental results of neutron induced fission of ^{238}U were used. The results of folding calculations using a parametrization based on averaging data of neutron induced fission of several uranium isotopes are, within the errors, identical with those obtained from ^{238}U(n,f) alone.

In good agreement with the experimental data a proton odd-even-effect δ_{calc} = $(7.1 \pm 1.5)\%$ and a peak-to-valley ratio $p = 7.6 \pm 2.6$ was obtained from the folding calculations which included the excitation of the double GDR. Calculations where the excitation of the double GDR was not taken into account result in a peak-to-valley ratio p of 16.2 ± 3.2 and an odd-even-effect δ_{calc} of $(9.0 \pm 1.5)\%$. In this case, the peak-to-valley ratio is not compatible with the experimental results as can be seen in Fig. 9. Therefore, our data give evidence for the excitation of the double giant-dipole resonance in uranium. This result is in good agreement with recently reported neutron removal cross sections of ^{238}U [14]. In that publication it was shown that the cross sections for 1n-4n removal are well reproduced by similar WW calculations which use the same parametrization of the fission probability.

5 Conclusion

We measured the cross sections for electromagnetic fission of uranium projectiles at E/A = 600 and 1000 MeV for various targets. Fission events were selected by the requirements that the charge sum equaled 92 and no light charged particles from the interaction zone were detected. The small remaining nuclear background was determined using the method of factorization. Due to the selectivity of the applied experimental method small systematic errors were achieved. Comparisons between the data and Weizsäcker-Williams calculations including E1 and E2 excitations show good agreement. The calculated excitation function between E/A = 100 and 1000 MeV describes well most of the measured electromagnetic fission cross sections from different experiments. Weizsäcker-Williams calculations using the BCV parametrization for the cutoff parameter can better reproduce the experimental electromagnetic fission cross sections than calculations using the Kox parametrization.

Studies of the proton odd-even-effect and of the asymmetry of the charge distribution in comparison with folding calculations using the excitation energy distribution of the Weizsäcker-Williams calculations give evidence for the excitation of the double GDR. This is in good agreement with the recently reported 1n-4n removal cross sections of ^{238}U [14].

Due to the large cross sections, electromagnetic fission of heavy projectiles is a suitable tool to study fission at low excitation energies including fissile nuclei like isotopes produced in secondary beam experiments [17, 18].

Acknowledgement. The authors would like to thank T. Aumann and C. A. Bertulani for interesting and helpful discussions. J.P. and M.B. acknowledge the financial support of the Deutsche Forschungsgemeinschaft under the Contract No. Po256/2-1 and No. Be1634/1-1, respectively. This work was supported in part by the European Community under contract ERBCHGE-CT92-0003 and ERBCIPD-CT94-0091.

References

1. Norbury, J. W.: Phys. Rev. C **43**, R368 (1991) and references therein
2. Artru, X., Yodh, G.B.: Phys. Lett. **40B**, 43 (1972)
3. Heckman, H.H., Lindstrom, P.J.: Phys. Rev. Lett. **37**, 56 (1976)
4. Olsen, D.L., Berman, B.L., Greiner, D.E., Heckman, H.H., Lindstrom, P.J., Westfall, G.D., Crawford, H.J.: Phys. Rev. C **24**, 1529 (1981)
5. Mercier, M.T., Hill, J.C., Wohn, F.K., Smith, A.R.: Phys. Rev. Lett. **52**, 898 (1984)
6. Mercier, M.T., Hill, J.C., Wohn, F.K., McCullough, C.M., Nieland, M.E., Winger, J.A., Howard, C.B., Renwick, S., Matheis, D.K., Smith, A.R.: Phys. Rev. C **33**, 1655 (1986) and references therein
7. Aumann, T., Kratz, J.V., Stiel, E., Sümmerer, K., Brüchle, W., Schädel, M., Wirth, G., Fauerbach, M., Hill, J.C.: Phys. Rev. C **47**, 1728 (1993)
8. Hill, J.C., Wohn, F.K., Schwellenbach, D.D., Smith, A.R.: Phys. Lett. B **273**, 371 (1991)
9. Ritman, J., Berg, F.-D., Kühn, W., Metag, V., Novotny, R., Notheisen, M., Paul, P., Pfeiffer, M., Schwalb, O., Löhner, H., Venema, L., Gobbi, A., Herrmann, N., Hildenbrand, K.D., Mösner, J., Simon, R.S., Teh, K., Wessels, J.P., Wienold, T.: Phys. Rev. Lett. **70**, 533 (1993) and Phys. Rev. Lett. **70**, 2659 (1993)
10. Schmidt, R., Blaich, Th., Elze, Th.W., Emling, H., Freiesleben, H., Grimm, K., Henning, W., Holzmann, R., Keller, J.G., Klingler, H., Kulessa, R., Kratz, J.V., Lambrecht, D., Lange, J.S., Leiffels, Y., Lubkiewicz, E., Moore, E.F., Wajda, E., Prokopowicz, W., Schütter, Ch., Spies, H., Stelzer, K., Stroth, J., Walus, W., Wollersheim, H.J., Zinser, M., Zude, E.: Phys. Rev. Lett. **70**, 1767 (1993)
11. Wajda, E., Stroth, J., Blaich, Th., Elze, Th.W., Emling, H., Freiesleben, H., Grimm, K., Henning, W., Holzmann, R., Klingler, H., Kulessa, R., Kratz, J.V., Lambrecht, D., Leiffels, Y., Lubkiewicz, E., Moore, Stelzer, K., Walus, W., Zinser, M., Zude, E.: Nucl. Phys. A **569**, 141c (1994)
12. Aumann, T., Bertulani, C.A., Sümmerer, K.: Phys. Rev. C **51**, 416 (1995)
13. Emling, H.: Prog. Part. Nucl. Phys. Vol. 33, 729 (1994) and references therein
14. Aumann, T., Sümmerer, K., Geissel, H., Blank, B., Brohm, T., Clerc, H.-G., Czajkowski, S., Donzaud, C., Grewe, A., Hanelt, E., Heinz, A., Irnich, H., de Jong, M., Junghans, A., Magel, A., Münzenberg, G., Nickel, F., Pfützner, M., Piechaczek, A., Röhl, C., Scheidenberger, C., Schwab, W., Schmidt, K.-H., Steinhäuser, S., Trinder, W., Voss, B.: Z. Phys. A, in print (1995)
15. Jain, P.L., Aggarwal, M.M., El-Nagdy, M.S., Ismail, A.Z.M.: Phys. Rev. Lett. **52**, 1763 (1984)
16. Greiner, D.E., Crawford, H., Lindstrom, P.J., Kidd, J.M., Olson, D.L., Schimmerling, W., Symons, T.J.M.: Phys. Rev. C **31**, 416 (1985)
17. Schmidt, K.H., Heinz, A., Clerc, H.-G., Blank, B., Brohm, T., Czajkowski, S., Donzaud, C., Geissel, H., Hanelt, E., Irnich, H., Itkis, M.C., de Jong, M., Junghans, A., Magel, A., Münzenberg, G., Nickel, F., Pfützner, M., Piechaczek, A., Röhl, C., Scheidenberger, C., Schwab, W., Steinhäuser, S., Sümmerer, K., Trinder, W., Voss, B., Zhdanov, S.V.: Phys. Lett. B **325**, 313 (1994)
18. Bernas, M., Czajkowski, S., Armbruster, P., Geissel, H., Dassagne, Ph., Donzaud, C., Faust, H.-R., Hanelt, E., Heinz, A., Hesse, M., Kozhuharov, C., Miehe, Ch., Münzenberg, G., Pfützner, M., Röhl, C., Schmidt, K.-H., Schwab, W., Stéphan, C., Sümmerer, K., Tassan-Got, L., Voss, B.: Phys. Lett. B **331**, 19 (1994)
19. Justice, M., Blumenfeld, Y., Colonna, N., Delis, D.N., Guarino, G., Hanold, K., Meng, J.C., Peaslee, G.F., Wozniak, G.J., Moretto, L.G.: Phys. Rev. C **49**, R5 (1994)
20. Polikanov, S., Brüchle, W., Folger, H., Jäger, E., Krogulski, T., Schädel, M., Schimpf, E., Wirth, G., Aumann, T., Kratz, J.V., Stiel, N., Trautmann. N.: Z. Phys. **A** 350, 221 (1994)
21. Hubele. J., Kreutz, P., Adloff, J.C., Begemann-Blaich, M., Bouissou, P., Imme, G., Iori, I., Kunde, G.J., Leray, S., Lindenstruth, V., Liu, Z., Lynen, U., Meijer, R.J., Milkau, U., Maroni, A., Müller, W.F.J., Ngô, C., Ogilvie, C.A., Pochodzalla, J., Raciti, G., Rudolf, G., Sann, H., Schüttauf, A., Seidel, W., Stuttge, L., Trautmann, W., Tucholski, A.: Z. Phys. A **340**, 263 (1991)
22. Blaich, Th., Elze, Th.W., Emling, H., Freiesleben, H., Grimm, K., Henning. W., Holzmann, R., Ickert, G., Keller, J.G., Klingler, H., Kneissl, W., König, R., Kulessa, R., Kratz, J.V., Lambrecht, D., Lange, J.S., Leifels, Y., Lubkiewicz, E., Proft, M., Prokopowicz, W., Schütter, C., Schmidt, R., Spies, H., Stelzer, K., Stroth, J., Walus, W., Wajda, E., Wollersheim, H.J., Zinser, M., Zude, E.: Nucl. Inst. Meth. A **314**, 136 (1992)
23. Wilke, W., Kneissl, U., Weber, Th., Ströher, H., Cardman, L.S., Debevec, P.T., Hoblit, S.D., Jones, R.T., Nathan, A.M.: Phys. Rev. C **42**, 2148 (1990)
24. Fermi, E.: Z. Phys. **29**, 315 (1924)
25. von Weizsäcker, C.F.: Z. Phys. **88**, 612 (1934)
26. Williams, E.J.: Phys. Rev. **45**, 729 (1934)
27. Bertulani, C.A., Baur, G.: Phys. Rep. **163**, 299 (1988)
28. Norbury, J.W.: Phys. Rev. C **41**, 372 (1990) and Phys. Rev. C **42**, 711 (1990)
29. Veysièrre, A., Beil, H., Bergère, R., Carlos, P., Lepretre, A. and Kernbath, K.: Nucl. Phys. A **199**, 45 (1973)
30. Ries, H., Mank, G., Drexler, J., Heil, R., Huber, K., Kneissl, U., Ratzek, R., Ströher, H., Weber, T., Wilke, W.: Phys. Rev. C **29**, 2346 (1984)
31. Weber, Th., Heil, R.D., Kneissl, U., Wilke, W., Kihm, Th., Knöpfle, K.T., and Emrich, H.J.: Nucl. Phys. A **510**, 1 (1990)
32. Gurevich, G.M., Lazareva, L.E., Mazur, V.M., Solodukhov, G.V., Tulupov, B.A.: Nucl. Phys. A **273**, 326 (1976)
33. Pitthan, R., Buskirk, F.R., Houk, W.A., Moore, R.W.: Phys. Rev. C **21**, 28 (1980)

34. Caldwell, J.T., Dowdy, E.J., Berman, B.L., Alvarez, R.A., Meyer, P.: Phys. Rev. C **21**, 1215 (1980)
35. Reisdorf, W., Schädel, M.: Z. Phys. A **343**, 47 (1992)
36. Llope, W.J., Braun-Munzinger, P.: Phys. Rev. C **41**, 2644 (1990) and Phys. Rev. C **45**, 799 (1992)
37. Baur, G., Bertulani, C.A.: Phys. Rev. C **34**, 1654 (1986)
38. Benesh, C.J., Cook, B.C., Vary, J.P.: Phys. Rev. C **40**, 1198 (1989)
39. Kox, S., Gamp, A., Perrin, C., Arvieux, J., Bertholet, R., Bruandet, J.F., Buenerd, M., Cherkaoui, R., Cole, A.J., El-Masri, Y., Longequeue, N., Menet, J., Merchez, F., Viano, J.B.: Phys. Rev. C **35**, 1678 (1987)
40. Bertulani, C.A.: Phys. Lett. B **319**, 421 (1993)
41. Verboven, M., Jacobs, E., De Frenne, D.: Phys. Rev. C **49**, 991 (1994)
42. Wagemans, C.: The Nuclear Fission Process. Boca Raton, Ann Arbor, Boston, London: CRC Press 1991
43. Binns, W.R., Garrad, T.L., Israel, M.H., Kertzmann, M.P., Klarmann, J., Stone, E.C., Waddington, C.J.: Phys. Rev. C **36**, 1870 (1987)
44. Webber, W.R., Kish, J.C., Schrier, D.A.: Phys. Rev. C **41**, 520 (1990)
45. He, Y.D., Price, P.B.: Z. Phys. A **348**, 105 (1994)
46. Olsen, D.L., Berman, B.L., Greiner, D.E., Heckman, H.H., Lindstrom, P.J., Crawford, H.J.: Phys. Rev. C **28**, 1602 (1983)
47. Nethaway, D.R., Mendoza, B.: Phys. Rev. C **6**, 1827 (1972)
48. Nagy, S., Flynn, K.F., Gindler, J.E., Meadows, J.W., Glendenin, L.E.: Phys. Rev. C **17**, 163 (1978)
49. Gindler, J.E., Glendenin, L.E., Henderson, D.J., Meadows, J.W.: Phys. Rev. C **27**, 2058 (1983)
50. Pommé, S., Jacobs, E., Persyn, K., De Frenne, D., Govaert, K., Yoneama, M.-L.: Nucl. Phys. A **560**, 689 (1993)

This article was processed by the author using the LaTeX style file *pljour2* from Springer-Verlag.